Journal of Materials Chemistry

Cite this: J. Mater. Chem., 2012, 22, 8431

www.rsc.org/materials

PAPER

High capacity carbon dioxide adsorption by inexpensive covalent organic polymers†

Hasmukh A. Patel,[a] Ferdi Karadas,[b] Ali Canlier,[a] Joonho Park,[a] Erhan Deniz,[b] Yousung Jung,[a] Mert Atilhan*[b] and Cafer T. Yavuz*[a]

Received 8th February 2012, Accepted 21st February 2012
DOI: 10.1039/c2jm30761h

Efficient CO_2 scrubbing without a significant energy penalty remains an outstanding challenge for the fossil fuel-burning industry where aqueous amine solutions are still widely used. Porous materials have long been evaluated for next generation CO_2 adsorbents. Porous polymers, robust and inexpensive, show promise as feasible materials for the capture of CO_2 from warm exhaust fumes. We report the syntheses of porous covalent organic polymers (COPs) with CO_2 adsorption capacities of up to 5616 mg g^{-1} (measured at high pressures, *i.e.* 200 bar) and industrially relevant temperatures (as warm as 65 °C). COPs are stable in boiling water for at least one week and near infinite CO_2/H_2 selectivity is observed.

Introduction

One of the most pronounced impacts of climate change is carbon dioxide (CO_2) induced ocean acidification, leading, it is expected,[1] to corals and marine organisms, particularly pteropods, losing their aragonite shells. Despite the promise of some well-studied porous materials,[2] CO_2 scrubbing operations at fossil fuel-burning power plants continue to be reliant on aqueous organic amine solutions, *e.g.*, monoethanolamine[3] (MEA). Hybrid structures have emerged as promising alternatives[4] where framework structures offer chemospecific tailoring of the adsorptive surfaces.[5] Although covalent organic frameworks (COFs) offer light-weight porous alternatives for enhancing the per mass sorption in gas capture operations,[6] their measured CO_2 capacities fall short of reaching the theoretical predictions[7] of 9285 mg g^{-1} plus their instability in water can only be slowed down by alkylating the organic struts.[8] The cost of their production is also considerably higher than conventional porous solids. Although wholly organic polymers are known to be inexpensive and robust,[2] their disordered nature prohibits control over host–guest interactions and porous architecture, a significant drawback when ordered structure is a priority. A porous organic framework is generally constructed *via* a building-block approach by chemically binding monomer units with proper functional groups. For example, a series of COFs have been prepared by reacting hydroxyl-benzene derivatives with aryl boronic acids resulting in porous crystalline structure with high surface area.[9] COFs are shown to have promising gas capture behavior[6] stimulating renewed interest in porous organic network polymers.[10] To name a few, MOPs,[11] HCPs,[12] CMPs[13] by Cooper, PIMs[14] by Budd and McKeown, FDUs[15] by Zhao, CTFs[16] by Antonietti and Thomas, PAFs[17] by Zhu, PPNs[18] by Zhou, POFs[19] by Kanatzidis and BILPs[20] by El-Kaderi show notable gas capture and storage capacities. Specifically, PPN-4[18] shows the highest CO_2 capacity of porous polymers (2121 mg g^{-1} at 50 bar and 298 K) as well the highest ever surface area reported to date (6461 m^2 g^{-1}).

In any carbon capture and storage (CCS) and reuse scenario, the CO_2 capacity of the sorbent is the prime target rather than the intrinsic properties, such as surface area.[21] For a post-combustion application, 3 mmol g^{-1} CO_2 capacity at temperatures between 40 and 60 °C and pressures less than 6 bar are deemed to be ideal.[22] Pre-combustion CO_2 conditions are set at higher pressures, *e.g.*, a water–gas shift reaction produces[23] a mixture of H_2 (61.5%) and CO_2 (35.5%) at 30 bar. Pipeline compression of crude natural gas reaches[24] up to pressures in excess of 175 bar while CO_2 transport for sequestration demands[3] pressures of 150 bar. Liquefied natural gas (LNG) stack temperatures have to be limited to a maximum of 180 °C by regulations.[25] Ideally, a sorbent should tolerate all these conditions (0–175 bar and 40–180 °C), while retaining its CO_2 capacity.

Most natural gas processing plants offer the option to selectively capture and remove CO_2 from the syngas stream prior to combustion and electricity generation, called as pre-combustion capture stage.[26] The current state of the art technologies for the capture of CO_2 from natural gas derived syngas are based on physical solvent washing systems, for example Rectisol[27] and

[a]*Graduate School of EEWS (WCU), Korea Advanced Institute of Science and Technology (KAIST), Daejeon 305-701, Republic of Korea. E-mail: yavuz@kaist.ac.kr; Fax: +82 42 350 2248; Tel: +82 42 350 1718*
[b]*Department of Chemical Engineering, Qatar University, 2713 Doha, Qatar. E-mail: mert.atilhan@qu.edu.qa; Fax: +974 4403 2491; Tel: +974 4403 4142*

† Electronic supplementary information (ESI) available: Detailed information and discussion on synthesis, characterisation and theoretical calculations. See DOI: 10.1039/c2jm30761h

Selexol[28] processes. Both of these technologies are mature technologies that are currently being demonstrated in large scale natural gas processing and gasification plants. As an alternative method for CO_2 capture, adsorption can be considered to be one of the more promising methods, offering potential energy savings compared to absorbent systems, especially with respect to expensive thermal regeneration costs.[29] Pressure swing adsorptions (PSAs) using solid sorbents are known to be superior to temperature swing adsorptions (TSA) due to their rapid cycles, low energy requirements and capital investment costs.[30,31]

In this paper, we introduce covalent organic polymers (COPs), a new family of porous polymers that show high CO_2 capture capacity. COPs differ greatly from regular chain macromolecules since no post-processing or no cross-linking is necessary to attain their permanent porosity. COPs reported herein withstand boiling water for weeks without losing any capture capacity and show 100% recyclability at high pressures (up to 200 bar) and warm temperatures (as high as 65 °C).

Experimental

Materials and methods

Cyanuric chloride (CC), *N*,*N*-diisopropylethylamine (DIPEA), piperazine (anhydrous) and 4,4′-bipiperidine were purchased from Sigma-Aldrich, USA. 1,4-Dioxane and ethyl alcohol (EtOH) were purchased from SAMCHUN, South Korea. All solvents were dried and stored in anhydrous conditions before utilization in the synthesis.

Synthesis of COP-1. DIPEA (18.9 mL, 108.4 mmol) was added to piperazine (3.73 g, 43.3 mmol) dissolved in 1,4-dioxane (150 mL) at 288 K. Cyanuric chloride (5.00 g, 27.1 mmol) dissolved in 1,4-dioxane (50 mL) was added dropwise to the above solution with continuous stirring at 15 °C in an N_2 environment. The white precipitate was stirred at 15 °C for 1 h, before being stirred at 25 °C for 2 h and then at 85 °C for 21 h. The off-white precipitate was washed with 1,4-dioxane and soaked in EtOH three times over the period of 12 h. Finally, the precipitate was dried at room temperature under vacuum for 2 h. Yield: 86%. Elemental analysis for $C_7N_5H_7$ calculated (%): C, 52.2; H, 4.4; N, 43.5. Found (%): C, 54.2; H, 6.2; N, 39.6. See ESI† for more details on methods and characterization.

Synthesis of COP-2. DIPEA (1.5 mL, 8.6 mmol) was added to 4,4′-bipiperidine (0.46 g, 2.7 mmol) dissolved in 1,4-dioxane (80 mL) at 15 °C. Cyanuric chloride (0.30 g, 1.6 mmol) dissolved in 1,4-dioxane (10 mL) was added dropwise to the above solution with continuous stirring at 15 °C in an N_2 environment. The white precipitate was stirred at 15 °C for 1 h, before being stirred at 25 °C for 2 h and then at 85 °C for 21 h. The white precipitate was washed with 1,4-dioxane and soaked in EtOH three times over the period of 12 h. Finally, the precipitate was dried at room temperature under vacuum for 2 h. Yield: 83%. Elemental analysis for $C_{13}N_5H_{18}$ calculated (%): C, 64; H, 7.4; N, 28.7. Found (%): C, 64.7; H, 7.6; N, 27.6. See ESI† for more details on methods and characterization.

Characterisation

CHN analyses were performed on an elemental analyser ThermoQuest Italia S.P.A (CE instrument). FT-IR spectra were recorded as KBr pellet using a Perkin-Elmer FT-IR spectrometer. ^1H and ^{13}C NMR spectra were recorded on a Bruker DMX400 NMR spectrometer. Solid-state cross-polarization magic angle spinning (CP/MAS) NMR spectra were recorded on a Bruker Avance III 400 WB NMR spectrometer. Thermogravimetric analysis (TGA) was performed on a NETZSCH-TG 209 F3 instrument by heating the samples to 800 °C at 10 °C min^{-1} in N_2 or air atmosphere. N_2 sorption isotherms were obtained with a Micromeritics ASAP 2020 accelerated surface area and porosimetry analyzer at 77 K. Prior to analysis, the samples were degassed at 150 °C for 5 h under vacuum. The adsorption–desorption isotherms were evaluated to give the pore parameters, including BET surface area, pore size, and pore volume. X-Ray diffraction (XRD) patterns of the samples were acquired from 0.5 to 60° by a Rigaku D/MAX-2500 (18 kW) Micro-area X-ray diffractometer. See ESI† for more details on methods and characterisation.

Theoretical simulations

Theoretical CO_2 capture capacities were determined by Cerius2 v. 4.0 software (Accelrys Software Inc., San Diego, CA, USA). The force field (FF) parameters and charges for CO_2 were adapted from J. G. Harris and K. H. Yung,[32] and those for COPs were obtained from Dreiding2.21 and the equilibrium charge method in Cerius2. The amorphous polymer frame of COP-1 was prepared by using a building module in Cerius2. To calculate the available volume, the probe radius of 1.4 Å was used. See ESI† for more details and discussion.

Gas sorption measurements

Low-pressure CO_2 and N_2 adsorption–desorption isotherms were measured at 273 K using a static volumetric system (ASAP 2020, Micromeritics Inc., USA). Prior to adsorption measurements, the samples were dried at 423 K at a heating rate of 1 K min^{-1} under vacuum (5×10^{-3} mmHg) for 5 h. High-pressure hydrogen adsorption measurements at 298 K up to 100 bar were carried out in an automated high pressure gas adsorption system BELSORP-HP, BEL Japan, Inc. Prior to the sorption isotherm measurements, samples were activated at a heating rate of 1 K min^{-1}, to 423 K under vacuum (6.7×10^{-2} Pa). A Rubotherm® Magnetic Suspension Balance[33] was utilized for high pressure CO_2 adsorption capacity determination. In a typical high pressure CO_2 adsorption–desorption isotherm measurement, approximately 0.25 g of COP was placed on a holder that was previously activated at 423 K. The system is taken under vacuum for 24 h at 336 K. CO_2 is pressurized *via* a Teldyne Isco 260D fully automated gas booster and charged into the high-pressure cell. CO_2 adsorption–desorption isotherms at 318, 328 and 338 K up to 200 bars were measured. See ESI† for more details on methods and characterization.

Results and discussion

We show that a theoretically rationalized (Fig. 1) amorphous porous polymer (COP-1, Fig. 2) reveals a CO_2 capacity of

5616 mg g^{-1} (Table 1). Another covalent organic polymer (COP-2) shows near infinite CO_2/H_2 selectivity (Fig. 3). These COPs were found to be extremely robust (Fig. 4), showing no deterioration even after boiling in H_2O for over a week.

Triazines[16] offer high nitrogen content, a desirable feature[34] for CO_2-specific gas operations. By coupling with mono-protic divalent nucleophiles (*e.g.*, piperazine), 2,4,6-trichloro-1,3,5-triazine (commonly known as cyanuric chloride or CC)[35] forms extended polymer networks, hereafter named as covalent organic polymers (COPs) (see Experimental section above and ESI† for extensive details on synthesis and characterization of COPs). Secondary amines produce COPs with tertiary nitrogens that are well suited for reversible CO_2 binding.

We simulated an amorphous COP (Fig. 1) with respect to its preferential CO_2 binding capacity at elevated pressures. As the density of amorphous COP-1 was found to be 0.127 g mL^{-1}, the CO_2 capacity is expected to be significantly high. Gravimetric analysis through a Magnetic Suspension Balance (MSB) offers precise measurements[33,36] with a wide range of pressures (UHV-350 bar) and temperatures (−196 to 350 °C) while maintaining ambient environment for the balance. When subjected to high pressures (up to 200 bar) in a MSB setup, nitrogen rich (40% w/w) COP-1 yields a remarkably greater capacity of 5616 mg g^{-1} when compared with COP-2 that yields 2086 mg g^{-1}, although the latter exhibits nearly similar surface area of 168 m^2 g^{-1} and 158 m^2 g^{-1} respectively. Low pressure (up to 1 bar) CO_2 adsorptivities show (Fig. 3) an expected no-hysteresis pattern, indicating very minute chemisorptivity.

In the ^{13}C-NMR and ^{1}H-NMR spectra (see ESI†) of the COPs, the presence of aliphatic CH_2 group was confirmed from the ^{13}C chemical shift at 44.2 and 43 ppm for COP-1 and COP-2, respectively. The CH functionality in COP-2 shows another, but lower ^{13}C chemical shift at 29.3 ppm. The triazine ring carbons were assigned to 164.7 and 164.3 ppm in the ^{13}C NMR spectra of COP-1 and COP-2, respectively. The ^{1}H-NMR spectra show chemical shifts at 3.2 ppm which correspond to methylene groups of piperazine and bipiperidine in COP-1 and COP-2, respectively. The broad chemical shift in COP-2 can be attributed to the diverse interactions between CH and CH_2 groups of bipiperidine. The internal standard, TMS, shows the reference chemical shift at 0 ppm.

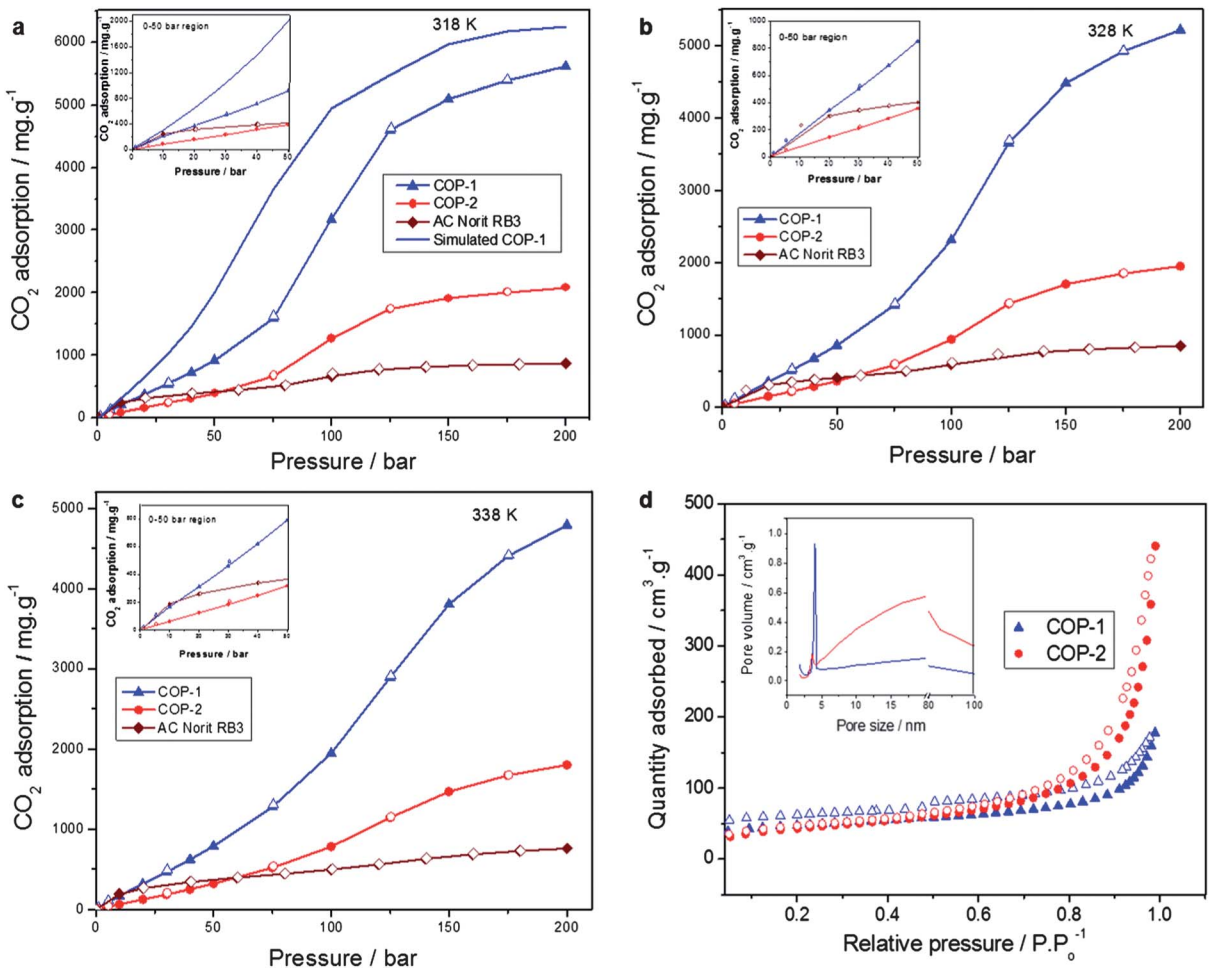

Fig. 1 High pressure (up to 200 bar) CO_2 and low pressure N_2 adsorptions for COPs. CO_2 adsorption (filled symbols)–desorption (open symbols) isotherms at (a) 318 K, (b) 328 K, and (c) 338 K measured with a Rubotherm® Magnetic Suspension Balance (inset: 0–50 bar region was magnified for better display). Theoretical simulation (colored straight line) shows a near fit to the experimental values. (d) N_2 adsorption-desorption isotherm measured at 77 K (inset: pore size *vs.* pore volume).

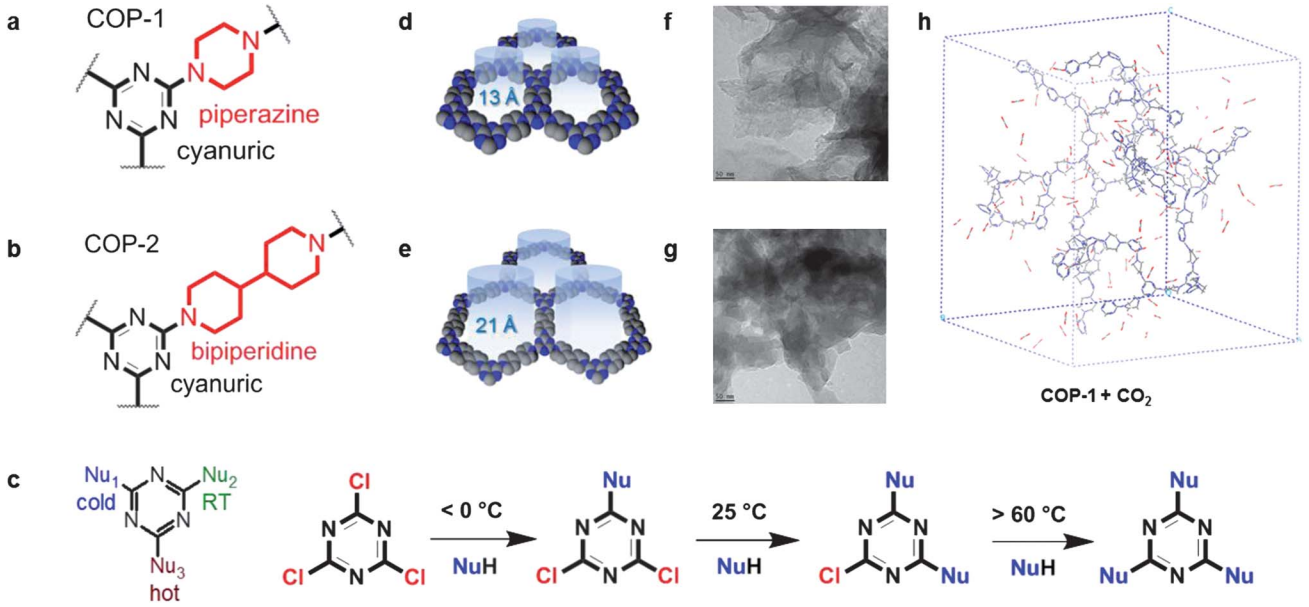

Fig. 2 Synthesis and characterization of COPs. A cold-to-reflux reaction of cyanuric chloride (CC) and a linker, piperazine for COP-1 (a) and 4,4′-bipiperidine for COP-2 (b), produced tens of grams overnight (c). Dioxane was found to be the best solvent (see ESI†) and *N*,*N*-diisopropylethylamine (DIPEA) was the preferred base. No post-synthetic workup or activation procedure was required. Conventional drying methods were used for gas adsorbent preparation. CC is known to exchange chlorides stepwise by temperature. Monoprotic nucleophiles (NuH) displace chlorides with the help of an aprotic base, while yielding intermediates. Calculated pore sizes are (d) COP-1: 13 Å and (e) COP-2: 21 Å. Experimental pore size averages are found to be larger but the theoretical order of the COPs w.r.t. each other fits well (Fig. 1d, inset). (f and g) Transmission electron micrographs (TEM) agree with the amorphous but flaky nature of the COP structures (scale bars are all 50 nm). (h) COP-1 (amorphous) was constructed by random assembly of rings into a 3D super structure. CO_2 was found to coagulate where rings are found (see ESI† for more theoretical discussion).

Table 1 Comparison of surface area, CO_2 capture and cost for selected adsorbers

	Surface area$_{BET}$		Total CO_2		
Material[a]	$m^2\ g^{-1}$	$mg\ g^{-1}$	*P* in bar	*T* in K	Materials cost[b] $ kg^{-1} CO_2
COP-1	168	5616	200	318	$9.8
		60	1	298	$917
COP-2	158	2086	200	318	$22 570
		41	1	298	$1 148 341
PPN-4 (ref. 26)	6461	2121	50	298	$78 287
		65	1	298	$2 554 584
PAF-1 (ref. 29)	5600	1585	40	298	$152 169
		45	1	298	$5 359 733
COF-102 (ref. 9)	3620	1200	55	298	$88 598
		68	1	298	$1 563 485
HCP-1 (ref. 12)	1646	585	30	298	$448
		75	1	298	$3493
BILP-1 (ref. 20)	1172	130	1	298	$693 129
POF1B (ref. 19)	917	92	1	298	$6761
MEA (ref. 30)	N/A	117	24	313	$68.4
		60	1	298	$133

[a] COP: covalent organic polymer, PPN: porous polymer network, PAF: porous aromatic framework, COF: covalent organic framework, HCP: hypercrosslinked polymers, BILP: benzimidazole-linked polymer, POF: porous organic framework, MEA: mono-ethanol amine in 15% w/w aqueous solution. [b] Materials costs were determined using a Sigma-Aldrich® 2009–2010 catalogue, in order to establish a fair comparison. Actual costs will be lower. Solvents and bases are considered to be fully recycled.

Functional groups present in COPs show characteristic FT-IR absorptions. In their respective FT-IR spectra, several strong bands in the 1200–1600 cm^{-1} region were identified corresponding to the typical stretching modes of CN heterocycles (see ESI†). Additionally, the characteristic breathing mode of the triazine units is evident around 800 cm^{-1}. The absorption band of saturated carbons of piperazine and 4,4′-bipiperidine are assigned near 2930 cm^{-1}. The absence of the characteristic C–Cl stretching vibration at 850 cm^{-1} confirmed that all three chlorine atoms on CC have been substituted.

Solvents are known to have direct impact[37] on the porosity of microporous polymers. Dioxane and THF are commonly chosen

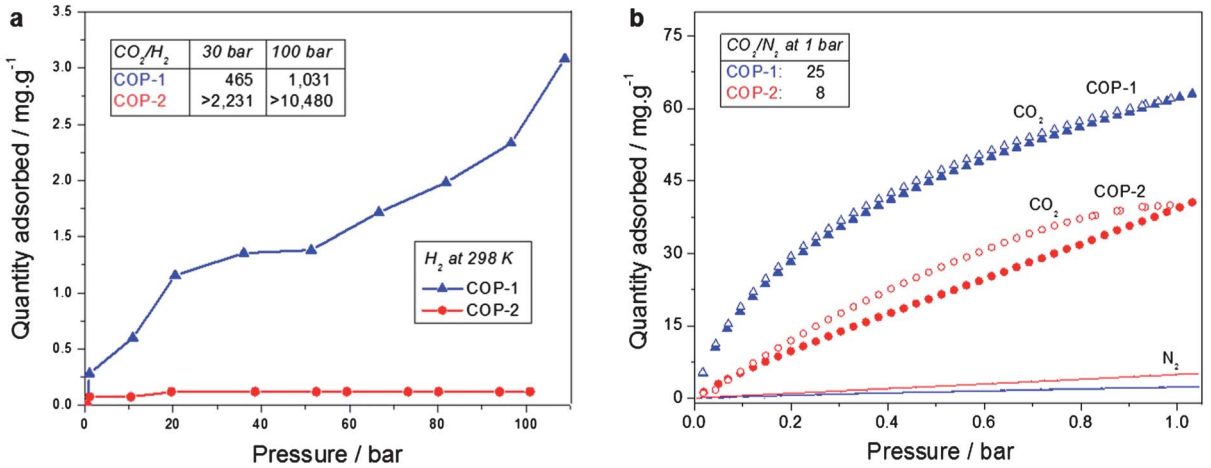

Fig. 3 High pressure (up to 100 bar) H_2 adsorption and low pressure (up to 1 bar) CO_2 and N_2 adsorption isotherms of COPs. (a) Hydrogen adsorption isotherms of COPs at 298 K. CO_2/H_2 selectivities at 30 bar (pre-combustion operation pressure) and 100 bar (maximum pressure in our system) are displayed in a table inside the figure. Selectivities are calculated from separate measurements of respective gases. COP-2 data were normalized since negative adsorptions were recorded in multiple experiments. With no measured adsorption, COP-2 shows near infinite selectivity to CO_2. (b) CO_2 adsorption isotherms (filled symbols), desorption isotherms (open symbols) and N_2 adsorption–desorption isotherms (lines) measured at 273 K. CO_2/N_2 selectivities at 1 bar were tabulated inside the figure using the respective, separate measurements.

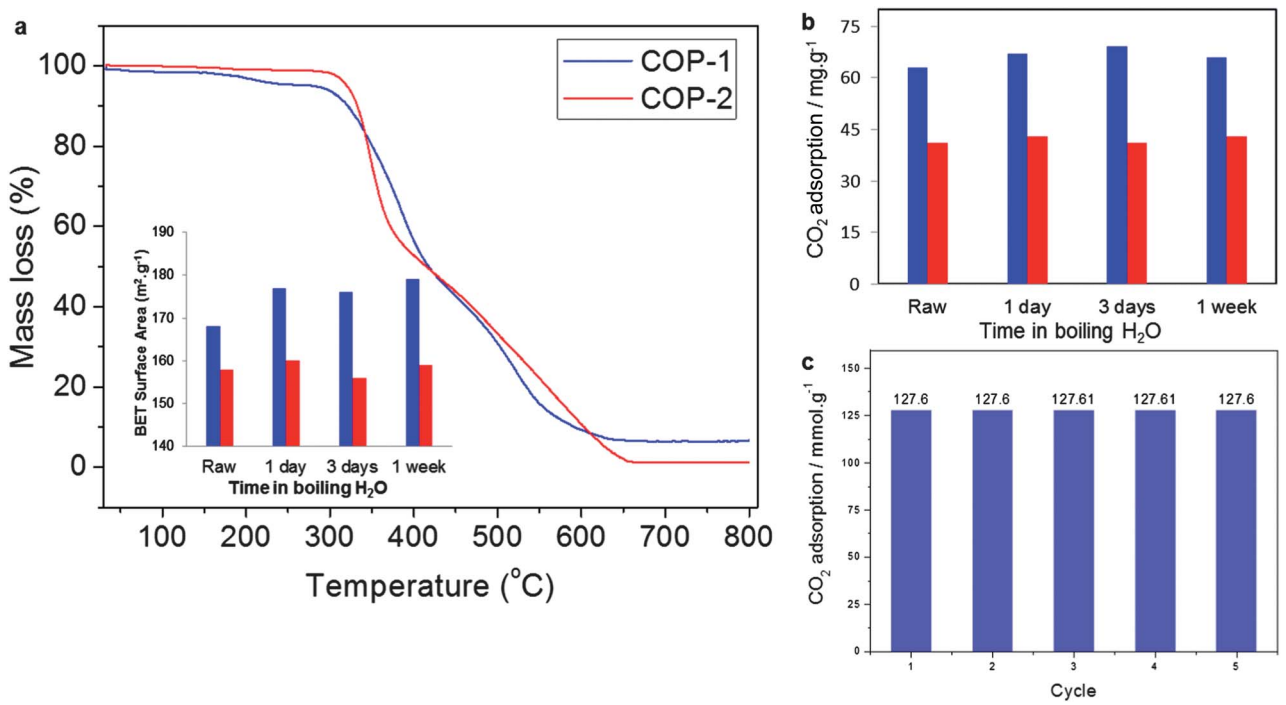

Fig. 4 Thermal stability and recyclability of COPs. (a) Thermogravimetric analysis of COPs in air. Inset: BET surface area change upon boiling COPs in H_2O (100 °C) for 1 day, 3 days and 1 week. A boiling water test was carried out by placing 100–300 mg of the sorbent in 15 mL of water and keeping it at 100 °C for the desired time. (b) Low pressure (1 bar) CO_2 adsorption capacities of COPs were unchanged over boiling in H_2O. (c) Multi-cycle study of high pressure CO_2 adsorption capacity for COP-1 at 318 K up to 200 bar. After each compression, system was depressurized to vacuum and allowed to be degassed completely.

as solvents in cyanuric acid based reactions[35] on account of their inert behavior towards the CC and linkers. Since the substitution of all three chlorides with the linkers used in this investigation was not possible below 85 °C, THF was found to be ineffective since its boiling point is 68 °C. Dimethyl acetamide, toluene and ethanol all react with cyanuric chloride, restricting the interaction of linkers and results in low surface area products. Table S1† shows the solvent effect on the surface area of COP-1.

COPs show low to no selectivity for H_2 (Fig. 3) when compressed up to 100 bar at RT. Owing to its large average pore sizes, COP-2 does not adsorb any H_2, leading to a near

infinite selectivity for CO_2 over H_2 and proving its promise for pre-combustion *syn*-gas mixtures (61.5% H_2, 35.5% CO_2) where high CO_2 selectivity over H_2 is desired.[23] Gas adsorptions are also found to be completely reversible with negligible hysteresis. Repetitive measurements using the same sample confirm 100% recyclability (Fig. 4) for at least five cycles.

All adsorption isotherms (Fig. 1) follow a Type IV or V Brunauer isotherm for both COPs.[38] Activated carbon Norit® RB3 shows a clean Type IV behavior, owing to a mechanism called capillary condensation. Although there is no experimental evidence, 3D COF structures have been simulated[7] to show similar Type IV isotherms for CO_2 adsorption. In the COPs reported herein, close to insignificant low-pressure saturations lead to isotherm assignments (Fig. 1) which fall in between Type IV and V. Judging from the lack of hysteresis, these findings can be attributed to weak interactions between CO_2 molecules and the sorbent for the most part. For example, the tertiary and aromatic nitrogens present in COP-1 are believed to be responsible for the complete reversibility. Reversible flexing[39] can also be operative, especially for the second "jump" in the isotherms (Fig. 1), since purely organic materials tend to show elastic behavior[36] on account of the rotational freedom of sp^3–sp^3 covalent bonds. Nitrogen content, however, enables enhanced capture for COP-1 at higher pressures where chemical affinity is the prime metric. COP-2 lacks the small pores, hence the low capacity at both high and low pressures. CO_2/N_2 selectivities of COP-1 and COP-2 are 25 and 7.9, respectively at 298 K and 1 bar, *cf.* 9–20 for Cooper's networks.[21]

The 77 K N_2 adsorption–desorption isotherms for COPs follow patterns similar to those for the low-pressure CO_2 adsorptions, yet they differ (Fig. 1) substantially in the higher relative pressure region. A continuous increase after the adsorption at low relative pressure, indicating an adsorption on the outer surface of small particles, is evident, especially so for COP-2, which exhibits a combination of Type I and II isotherms. The increase in the N_2 sorption at relative pressures above 0.9 is partly a consequence of inter-particulate porosity associated with the meso- and macrostructures of the samples and inter-particular voids. The apparent surface areas, calculated (Table 1, detailed porosity parameters are tabulated in the ESI†) from the Brunauer–Emmett–Teller (BET) model, are 168 and 158 $m^2\ g^{-1}$ for COP-1 and COP-2 respectively.

COPs are highly resistant to the extreme conditions, which commonly exist in exhaust streams. COP-1 and COP-2 were boiled in H_2O over days without losing (Fig. 4) any of their capacities or porosities. Also, when their solid samples were stored under ambient atmospheric conditions (no care was taken), no degradation was noted over several months. Thermal stability was observed up to 350 °C in air (Fig. 4) and 450 °C under N_2 (see ESI†).

Cost of the sorbent material has a direct impact on a CCS operation, as it is one of the leading factors for MEA's dominance in CCS plans.[3] Sustainability relies primarily on the treatment materials[40] and a low cost sorbent is almost always favoured, even if overall capacity needs to be compromised. COP-1 has a price tag as low as $10 per kg of CO_2 removed, significantly lower than many other popular CO_2 capture sorbents (Table 1).

Conclusion

In order to put these findings into perspective, COP-1 can hold up to more than five times the CO_2 present in dry ice. Considering that COPs show modest surface areas, yet yield exceptional capacities, there is enough evidence to believe that the world records can be broken if these structures are tuned even more so with respect to gas specific functionalities and porosities. Inevitably, new materials will emerge, as porous polymers continue to showcase significant promise for the development of efficient and robust CCS sorbents. The challenge, however, rests in designing materials with improved sustainability (esp. low cost) and stability (*e.g.* in hot water).[41]

Acknowledgements

This work was made possible by NPRP grant # 08-670-1-124 from the Qatar National Research Fund (a member of Qatar Foundation). The statements made herein are solely the responsibility of the authors. We also acknowledge the financial support by grants from Korea CCS R&D Center, funded by the Ministry of Education, Science and Technology of Korean government, and KAIST EEWS Initiative. YJ acknowledges the support from the NRF Korea (WCU-R31-2008-000-10055-0, 2010-0023018).

Notes and references

1 J. M. Pandolfi, S. R. Connolly, D. J. Marshall and A. L. Cohen, *Science*, 2011, **333**, 418–422.
2 A. Thomas, *Angew. Chem., Int. Ed.*, 2010, **49**, 8328–8344.
3 G. T. Rochelle, *Science*, 2009, **325**, 1652–1654.
4 S. Keskin, T. M. van Heest and D. S. Sholl, *ChemSusChem*, 2010, **3**, 879–891.
5 S. Ma and H.-C. Zhou, *Chem. Commun.*, 2010, **46**, 44–53.
6 H. Furukawa and O. M. Yaghi, *J. Am. Chem. Soc.*, 2009, **131**, 8875–8883.
7 Y. J. Choi, J. H. Choi, K. M. Choi and J. K. Kang, *J. Mater. Chem.*, 2011, **21**, 1073–1078.
8 L. M. Lanni, R. W. Tilford, M. Bharathy and J. J. Lavigne, *J. Am. Chem. Soc.*, 2011, **133**, 13975–13983.
9 A. P. Côté, A. I. Benin, N. W. Ockwig, M. O'Keeffe, A. J. Matzger and O. M. Yaghi, *Science*, 2005, **310**, 1166.
10 R. Dawson, A. I. Cooper and D. J. Adams, *Prog. Polym. Sci.*, 2012, **37**, 530–563.
11 R. Dawson, E. Stockel, J. R. Holst, D. J. Adams and A. I. Cooper, *Energy Environ. Sci.*, 2011, **4**, 4239–4245.
12 C. F. Martin, E. Stockel, R. Clowes, D. J. Adams, A. I. Cooper, J. J. Pis, F. Rubiera and C. Pevida, *J. Mater. Chem.*, 2011, **21**, 5475–5483.
13 R. Dawson, D. J. Adams and A. I. Cooper, *Chem. Sci.*, 2011, **2**, 1173–1177.
14 N. B. McKeown and P. M. Budd, *Macromolecules*, 2010, **43**, 5163–5176.
15 F. Zhang, Y. Meng, D. Gu, Y. Yan, C. Yu, B. Tu and D. Zhao, *J. Am. Chem. Soc.*, 2005, **127**, 13508–13509.
16 P. Kuhn, M. Antonietti and A. Thomas, *Angew. Chem., Int. Ed.*, 2008, **47**, 3450–3453.
17 T. Ben, H. Ren, S. Q. Ma, D. P. Cao, J. H. Lan, X. F. Jing, W. C. Wang, J. Xu, F. Deng, J. M. Simmons, S. L. Qiu and G. S. Zhu, *Angew. Chem., Int. Ed.*, 2009, **48**, 9457–9460.
18 D. Yuan, W. Lu, D. Zhao and H.-C. Zhou, *Adv. Mater.*, 2011, **23**, 3723–3725.
19 A. P. Katsoulidis and M. G. Kanatzidis, *Chem. Mater.*, 2011, **23**, 1818–1824.
20 M. G. Rabbani and H. M. El-Kaderi, *Chem. Mater.*, 2011, **23**, 1650–1653.

21 R. Dawson, E. Stockel, J. R. Holst, D. J. Adams and A. I. Cooper, *Energy Environ. Sci.*, 2011, **4**, 4239–4245.
22 M. L. Gray, K. J. Champagne, D. Fauth, J. P. Baltrus and H. Pennline, *Int. J. Greenhouse Gas Control*, 2008, **2**, 3–8.
23 D. M. D'Alessandro, B. Smit and J. R. Long, *Angew. Chem., Int. Ed.*, 2010, **49**, 6058–6082.
24 S. Mokhatab and M. J. Economides, *World Oil*, 2006, **227**, 95–99.
25 A. J. Kidnay and W. R. Parrish, *Fundamentals of Natural Gas Processing*, CRC Press, Boca Raton, Florida, 2006.
26 T. C. Drage, O. Kozynchenko, C. Pevida, M. G. Plaza, F. Rubiera, J. J. Pis, C. E. Snape and S. Tennison, *Energy Proc.*, 2009, **1**, 599–605.
27 H. Weiss, *Gas Sep. Purif.*, 1988, **2**, 171–176.
28 P. Chiesa, S. Consonni, T. Kreutz and W. Robert, *Int. J. Hydrogen Energy*, 2005, **30**, 747–767.
29 M. Radosz, X. Hu, K. Krutkramelis and Y. Shen, *Ind. Eng. Chem. Res.*, 2008, **47**, 3783–3794.
30 A. D. Ebner, M. L. Gray, N. G. Chisholm, Q. T. Black, D. D. Mumford, M. A. Nicholson and J. A. Ritter, *Ind. Eng. Chem. Res.*, 2011, **50**, 5634–5641.
31 M. G. Plaza, S. García, F. Rubiera, J. J. Pis and C. Pevida, *Chem. Eng. J.*, 2010, **163**, 41–47.
32 J. G. Harris and K. H. Yung, *J. Phys. Chem.*, 1995, **99**, 12021–12024.
33 F. Karadas, C. T. Yavuz, S. Zulfiqar, S. Aparicio, G. D. Stucky and M. Atilhan, *Langmuir*, 2011, **27**, 10642–10647.
34 N. Y. Du, H. B. Park, G. P. Robertson, M. M. Dal-Cin, T. Visser, L. Scoles and M. D. Guiver, *Nat. Mater.*, 2011, **10**, 372–375.
35 G. Blotny, *Tetrahedron*, 2006, **62**, 9507–9522.
36 S. Zulfiqar, F. Karadas, J. Park, E. Deniz, G. D. Stucky, Y. Jung, M. Atilhan and C. T. Yavuz, *Energy Environ. Sci.*, 2011, **4**, 4528–4531.
37 R. Dawson, A. Laybourn, Y. Z. Khimyak, D. J. Adams and A. I. Cooper, *Macromolecules*, 2010, **43**, 8524–8530.
38 D. M. Ruthven, *Principles of Adsorption and Adsorption Processes*, John Wiley & Sons, Inc., New York, 1984.
39 D. Tanaka, A. Henke, K. Albrecht, M. Moeller, K. Nakagawa, S. Kitagawa and J. Groll, *Nat. Chem.*, 2010, **2**, 410–416.
40 C. T. Yavuz, J. Mayo, C. Suchecki, J. Wang, A. Ellsworth, H. D'Couto, E. Quevedo, A. Prakash, L. Gonzalez, C. Nguyen, C. Kelty and V. Colvin, *Environ. Geochem. Health*, 2010, **32**, 327–334.
41 C. T. Yavuz, B. D. Shinall, A. V. Iretskii, M. G. White, T. Golden, M. Atilhan, P. C. Ford and G. D. Stucky, *Chem. Mater.*, 2009, **21**, 3473–3475.